View Article Online / Journal Homepage / Table of Contents for this issue

Ultrafast vibrational dynamics observed in higher electronic excited states of iodine using pump-UV DFWM spectroscopy

A. Scaria, V. Namboodiri, J. Konradi and A. Materny*

Received 12th October 2007, Accepted 19th November 2007
First published as an Advance Article on the web 10th December 2007
DOI: 10.1039/b715814a

Published on 10 December 2007. Downloaded by University of Pittsburgh on 27/10/2014 07:40:52.

By using a combination of an initial pump pulse and a degenerate four-wave mixing process, we show that an interrogation of the vibrational dynamics occurring in different electronic states of molecules is possible. The technique is applied to iodine. The initial pump pulse is used to populate the $B(^3\Pi_u^+)$ state of molecular iodine in the gas phase. Now, by using an internal time delay in the DFWM process, which is resonant with the transition between the B state and a higher lying ion-pair state, the vibrational dynamics of the B state and the ion-pair state could be observed. States of even symmetry are investigated, which are accessed by a one photon transition from the B state. By a proper choice of the wavelengths used for the pump and DFWM beams, the dynamics of ion-pair states belonging to two different tiers are monitored.

1. Introduction

Time-resolved nonlinear four-wave mixing (FWM) techniques have become valuable tools for investigating the dynamic properties of molecules.[1] FWM techniques like coherent anti-Stokes Raman scattering (CARS), degenerate four-wave mixing (DFWM), coherent Stokes Raman scattering (CSRS) and transient grating (TG) on a femtosecond time-scale have been used to gain information on different aspects of molecular dynamics in various systems.[2–8] CARS on a femtosecond time-scale was first employed by Leonhardt *et al.* to investigate the dynamics in condensed phase systems.[2,9] Later on, Hayden and Chandler applied the technique to gas phase systems where the dephasing times are much longer than in condensed phase systems.[10] The femtosecond DFWM technique was used by Motzkus *et al.* to replace the probe pulse in a pump–probe scheme to study unimolecular and bimolecular systems in the gas phase.[5] Schmitt *et al.* employed electronically resonant CARS and DFWM techniques to investigate vibrational dynamics in gas phase iodine.[3,4,11] By varying the time delay of one of the three pulses interacting with the sample, keeping the other two fixed, ground (X) and excited (B) state dynamics of iodine were probed. By choosing different polarizations for the three independent laser pulses interacting with the sample in a FWM scheme, Siebert *et al.* showed that a selectivity with respect to the vibrational and rotational dynamics could be achieved.[6] In the above studies the advantages of the FWM method including background free detection and use of different pulse ordering to obtain valuable information has been demonstrated.

In their experiment Motzkus *et al.* demonstrated that by the combination of an initial pump pulse and a DFWM process excited state dynamics of the molecules can be probed.[5] However, in these and similar studies by other researchers the FWM process was not in itself time-resolved. It appears to be attractive to make use of the FWM process in order to also gain information about higher lying excited states. A combination of this mere pump–probe technique with the method presented by Schmitt *et al.*[3,4,11] should be capable of accessing both electronic states involved in the resonant FWM transitions. In this contribution we present an application of a fully time-resolved combination of initial pump and DFWM to molecular iodine. Since iodine is well characterized by different spectroscopical techniques, it presents itself as an ideal model system.

In iodine there exist 20 ion-pair states dissociating into the ions I^+ and I^- compared with 23 valence states[12–14] where dissociation results in neutral atoms. These ion-pair states form three clusters each of six states and a single g–u pair. The first tier consisting of the six states $D'(2_g)$, $\beta(1_g)$, $D(0_g^+)$, $E(0_g^+)$, $\gamma(1_u)$, and $\delta(2_u)$ lies around 40 000 cm^{-1} above the ground state. These states correlate to the ions $I^-(^1S) + I^+(^3P_2)$. Above these, there is the second group of six states $(0_g^+, 0_u^+, 0_g^-, 0_u^-, 1_g, 1_u)$ lying around 47 000 cm^{-1} dissociating into the ions $I^-(^1S) + I^+(^3P_1, ^3P_0)$. The third cluster of six states dissociates into the ions $I^-(^1S) + I^+(^1D)$ and lies around 52 000 cm^{-1}. Ion-pair states in each tier are characterized by similar molecular constants and large equilibrium inter-nuclear distances. Since transitions between states are governed by selection rules and Franck–Condon factors, many of the ion pair states are not easily accessible. Taking into account the Hund's case (c), the allowed transitions for a one photon process are determined by the following selection rules

$$g \Leftrightarrow u,$$

$$\Delta\Omega = 0, \pm 1$$

$$0^+ \Leftrightarrow 0^+, 0^- \Leftrightarrow 0^-$$

Transitions from the ground state $(X\,^1\Sigma_g^+)$ to the ion-pair state using one photon correspond to large Franck–Condon shifts. Since the ground state of iodine possesses even symmetry, only

School of Engineering and Science, Jacobs University Bremen, Campus Ring 1, 28759 Bremen, Germany. E-mail: a.materny@jacobs-university.de

View Article Online

Published on 10 December 2007. Downloaded by University of Pittsburgh on 27/10/2014 07:40:52.

states of odd symmetry can be accessed by a single photon process. The valence to ion-pair transition obeys the $\Delta\Omega = 0$ selection rule. Although the transition to the $\Omega = 1$ state is allowed from the B state, it is approximately 30 times weaker than the $\Delta\Omega = 0$ transition.[15,16] The gerade states can be accessed by a one photon transition while to access the ungerade state, two photons are needed from the B state. There are different techniques used in the frequency domain to analyze these ion-pair states and several of these ion-pair states are characterized experimentally.[14] In most of these studies the excited B state is used as an intermediate state since it is readily accessible from the ground X state.

Even though extensive investigations on the ion-pair states have been performed in the frequency domain, only few time domain investigations are known.[17,18] To access higher lying ion pair states in iodine either multiphoton excitations or an excitation with vacuum ultraviolet (VUV) pulses have been used. By using multiphoton excitation techniques real-time wave packet motion on different potential energy surfaces was monitored by the group of Zewail.[17] Using this technique the authors were able to observe contributions from the $B\,^3\Pi_u{}^+$ state, the $D(0_u{}^+)$ state and the the repulsive $\Sigma(0_g^+)$ state. On the other hand Farmanara *et al.*[18] used femtosecond pulses in the VUV to excite coherent vibrational motion in the $D(0_u{}^+)$ ion-pair state. These techniques were successful in observing ion-pair states belonging to the first tier possessing odd symmetry.

Here, our question is whether the dynamics of the ion-pair states can be monitored using time-resolved FWM spectroscopy. By having different time ordering of the pulses involved in a resonant FWM process, ground as well as excited state dynamics can be accessed. To accomplish the goal of monitoring the ion-pair state, a two-step process has been devised for iodine, which uses an initial pump pulse to populate the B state followed by a time-resolved DFWM process to access the ion-pair states. This combination results in a (1 + 1) photon scheme where states of even symmetry belonging to the ion-pair states can be accessed and probed. In the pump-DFWM scheme the DFWM process follows an initial pump pulse and is hence capable of providing valuable information on the excited electronic states of the molecules. The initial pump pulse initiates the dynamics in the molecular system of interest, which is then interrogated by the DFWM process acting as probe. The initial pump in the visible is resonant with the ground to B state transition in iodine and the DFWM beams are resonant with the B to ion-pair state transition. Now by having different pulse sequences in the pump-DFWM scheme, wave packets on different potential energy surfaces can be prepared and their dynamics can be analyzed.

2. Experimental

The experimental setup used to realize the pump-DFWM scheme was as follows. A commercial femtosecond laser system (Clark-MXR Inc., CPA-2010) produces femtosecond pulses with a center wavelength of 775 nm at a repetition rate of 1 kHz. The pulses have a temporal width of 150 fs with an average energy of 1 mJ per pulse. In order to generate two different wavelengths for the pump-DFWM process, the output of the CPA was equally split to pump two optical parametric amplifiers (OPAs; TOPAS, Light Conversion). Wavelengths in the range 450–2700 nm could be generated from one of the OPAs while the other OPA covered wavelength ranges from 270–2700 nm. The OPA output covered the wavelength range required for the experiments. The output of one of the OPAs served as the initial pump pulse. The output of the other OPA was split into three equal parts, which formed the three four-wave mixing (FWM) beams. These laser pulses have pulse lengths of approximately 150 fs.

The FWM process requires a spatial and for the start of the experiment also a temporal overlap of the beams in the sample. The pulses were delayed during the course of the experiment, with respect to each other using computer controlled linear translation stages in Michelson interferometer arrangements. The temporal overlap of the beams is determined by using the optical Kerr effect[19] for ultraviolet beams. The positions of the delay stages at which the beams coincided in time was labeled as time-zero. The delay times mentioned in the following are always relative to this time-zero position. For the DFWM we have used the three-dimensional forward geometry (Folded BoxCARS),[20] which fulfils the phase matching condition and spatially separates the signal enabling a background-free detection. In this geometry the three beams will pass through the three corners of the front side of a box. After interaction with the sample, the signal emerges out from the fourth corner of the opposite box side. The initial pump is made to pass through the center of these box sides.

The four beams were focused into the cuvette containing iodine using a lens of focal length 200 mm. The cuvette was heated to approximately 60 °C to slightly increase the vapor pressure of the sample for a better signal. The spatially separated DFWM signal is filtered by a pinhole. The signal is then collimated using another lens of the same focal length and is finally directed into a single monochromator and after dispersion detected using a CCD camera. Since the signal is of the same wavelength as the incoming FWM beams, extreme care was taken to minimize background due to scattering from the walls of the cuvette. In the following, the results obtained from the experiments performed will be presented and the advantages of the technique in extracting molecular information will be discussed.

3. Results and discussion

Table 1 shows the molecular constants for the B state and the ion pair states belonging to the first tier and second tier that are relevant for the present study. These data are taken from the studies of Ishiwata and Tanaka.[21] Only states having an even symmetry and obeying the selection rule can be accessed from the B state. These states are shown in Table 1. The states

Table 1 Molecular constants for the excited iodine B state and the ion pair states relevant for the present study

State	T_e/cm^{-1}	ω_e/cm^{-1}
$B(^3\Pi_{0u}{}^+)$	15 641	127
$\beta(1_g)$	40 821	105
$E(0_g^+)$	41 411	101
$f(0_g^+)$	47 025	104
$G(1_g)$	47 559	106

 This journal is © the Owner Societies 2008

View Article Online

Published on 10 December 2007. Downloaded by University of Pittsburgh on 27/10/2014 07:40:52.

belonging to each tier have similar molecular parameters. The states $\beta(1_g)$ and $E(0_g^+)$ belong to the first tier while $f(0_g^+)$ and $G(1_g)$ belong to the second tier. The $\beta(1_g)$ and $E(0_g^+)$ states have been explored in the earlier experiments performed in the frequency domain by King *et al.*[22] by two photon sequential absorption spectroscopy and also by optical–optical double resonance experiments done by Perrot *et al.*[23]

The experimental methodology employed for the present study is depicted in Fig. 1. An initial pump pulse in the visible is used to populate the B state. The broad spectral band width of the femtosecond pulse creates a coherent superposition of several vibrational states (wave packet) in the B state. This wave packet is probed by a DFWM process the wavelength of which is resonant with the B to ion-pair state transition. DFWM involves the interaction of three laser beams of the same frequency with the sample, leading to the generation of a coherent fourth beam also of the same frequency. Both energy and momentum are conserved in this process. By varying the timing of one of the pulses involved in the DFWM process, the dynamics of the B state and the ion pair states can be obtained. A careful choice of the initial pump and FWM wavelengths is made to access ion-pair states belonging to two different tiers. Depending on the experiment, the wavelength of the initial pump was varied between 540–560 nm, which is in resonance with the ground ($X^1\Sigma_g^+$) to B state transition. The wavelength of the FWM excitation was varied in the range from 325 to 410 nm. This is in resonance with the transition from the B state to the lowest group of ion pair states. For the experiment each of the DFWM pulses possessed an average energy of 1.5 μJ pulse^{-1} while the initial pump pulse had an average energy of 3.5 μJ pulse^{-1}.

Different time ordering of the initial pump and DFWM pulses were employed to explore the dynamics of different excited states. A selective probing of the dynamics of the B state can be achieved if the DFWM process is not resolved in time. This is demonstrated here. For this, all the DFWM beams were made to arrive simultaneously. The initial pump pulse is scanned in time from negative to positive delay times. The dynamics is recorded as a function of delay time ΔT between the initial pump and the time-coincident DFWM pulses. Panel (a) of Fig. 2 shows the transient recorded for an initial pump wavelength of 560 nm and an FWM wavelength of 410 nm. The transients show well defined oscillations of the signal intensity with a period of approximately 388 fs for $\Delta T > 0$. For $\Delta T < 0$ a constant signal is observed. For negative time delays the time-coincident DFWM pulses are incident on the sample before the initial pump pulse. The constant signal thus observed is the weak non-resonant DFWM signal from the ground state. For positive time delays the initial pump arrives first. The spectrally broad initial pump pulse prepares a wave packet, which is oscillating in the bound B state. This is then probed by the time-delayed resonant DFWM pulses. Due to the presence of resonance a more

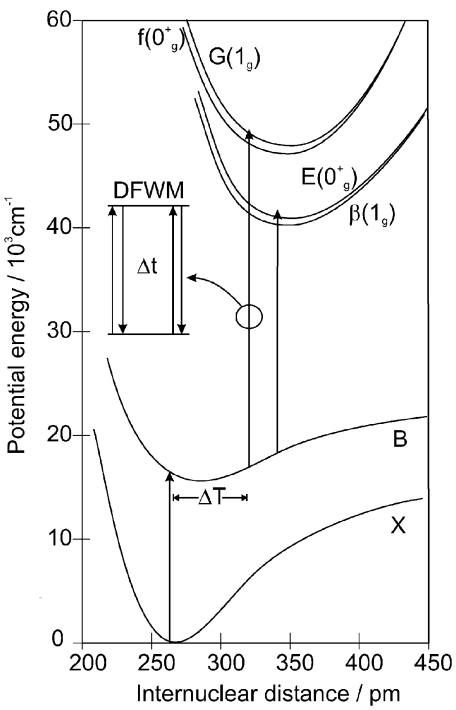

Fig. 1 Potential energy curves of molecular iodine relevant for the present study. Following the selection rules, the states $\beta(1_g)$ and $E(0_g^+)$ belonging to the first tier and the states $G(1_g)$ and $f(0_g^+)$ belonging to the second group are accessible from the excited B state.

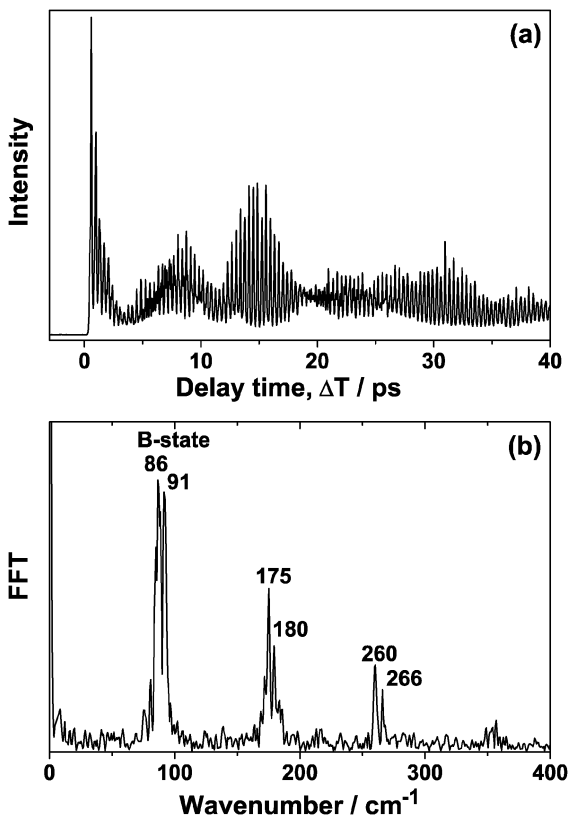

Fig. 2 Panel (a) shows the DFWM signal recorded as a function of the delay time ΔT between the initial pump (560 nm) and the three time-coincident FWM (410 nm) pulses. Transients show oscillations with a period of 388 fs. Panel (b) depicts the FFT spectrum of the transient in (a). It shows peaks in the region of 86 cm^{-1}, which correspond to the vibrational energy spacing of the B state of molecular iodine accessed by the 560 nm laser.

View Article Online

Published on 10 December 2007. Downloaded by University of Pittsburgh on 27/10/2014 07:40:52.

intense DFWM signal is observed. The transients for positive time delays thus reveal the dynamics of the excited B state. In order to analyze the data, a fast Fourier transform (FFT) of the transient is performed for positive time delays where the oscillations are observed. This is shown in panel (b) of Fig. 2. From the FFT it is clear that the oscillations are due to the superposition of vibrational eigenstates with an energy spacing of mainly 86 and 91 cm^{-1}. This corresponds well to the spacing between two vibrational states ($\Delta v' = 1$) in the B state[24] accessed by the 560 nm laser. Furthermore, the second harmonic ($\Delta v' = 2$) of these frequencies is observed at 175 and 180 cm^{-1}, while the third harmonic ($\Delta v' = 3$) is seen at 260 and 266 cm^{-1}.

The determination of the wave packet dynamics of the B state has been performed in the above experiment with time-coincident DFWM pulses. This will be useful in further experiments to separate the contributions of the B state and ion pair state in the recorded dynamics. In the second measurement, the initial pump pulse is made to arrive 42 ps earlier at the sample. This makes sure that part of the population is in the B state. Two (DFWM pump pulses pu_1 and pu_2) of the three FWM beams are kept temporally overlapped and fixed at time zero. The wavelength of the initial pump and DFWM beams is the same as in the previous experiments. The dynamics are recorded as a function of the time delay Δt between the third pulse (DFWM probe pulse pr) and the two time-coincident DFWM pump pulses. The transients for $\Delta t < 0$ and $\Delta t > 0$ are shown in panels (a) and (b) of Fig. 3, respectively. The modulations in the DFWM signal are observed for both positive and negative delay times. The FFT of the transient in (a) is shown in panel (c) of Fig. 3. The FFT of the transient for positive delay times is shown in panel (d) of Fig. 3.

The initial pump pulse and FWM probe together correspond to a photon energy of 42 247 cm^{-1} with which ion pair states belonging to the first tier are reached. As in the previous DFWM experiments performed on iodine,[4] we have to consider two scenarios. For $\Delta t < 0$ the probe pulse (pr) of the FWM process creates a wave packet in the higher lying ion pair state of iodine. This is then probed by the time delayed pump pulses (pu_1 and pu_2). The energy level diagram corresponding to this process is shown in panel (a) of Fig. 4. The transients in this case reveal the dynamics of the ion-pair state. The FFT of the transient in panel (a) is shown in panel (c) of Fig. 3. Along with the line at 86 cm^{-1}, which is the B state vibrational energy spacing there is a line at 98 cm^{-1}, which clearly belongs to the ion-pair state. This also matches well the spectroscopic constants listed in Table 1. The energy of the initial pump pulse and one of the FWM beams together is above the minima of $\beta(1_g)$ and $E(0_g^+)$, which are both accessible from the B state. A careful inspection of the FFT spectrum shown in panel (c) of Fig. 3 reveals that for negative delay time of the probe laser, B-state contributions are also observed. This is interesting since for $\Delta t < 0$ only ion pair state contributions are expected. However, here it should be noted that the investigations are performed on a population that is evolving in time. The initial pump pulse excites the molecules into the B state where a wave packet is created, which is oscillating back and forth. Now the first pulse (probe pulse) of the DFWM process interacts with this population. Since this probe pulse itself is varied in time there is a change of timing between the initial pump pulse and DFWM probe pulse. This results in the observation of the B state dynamics for negative time delays as well.

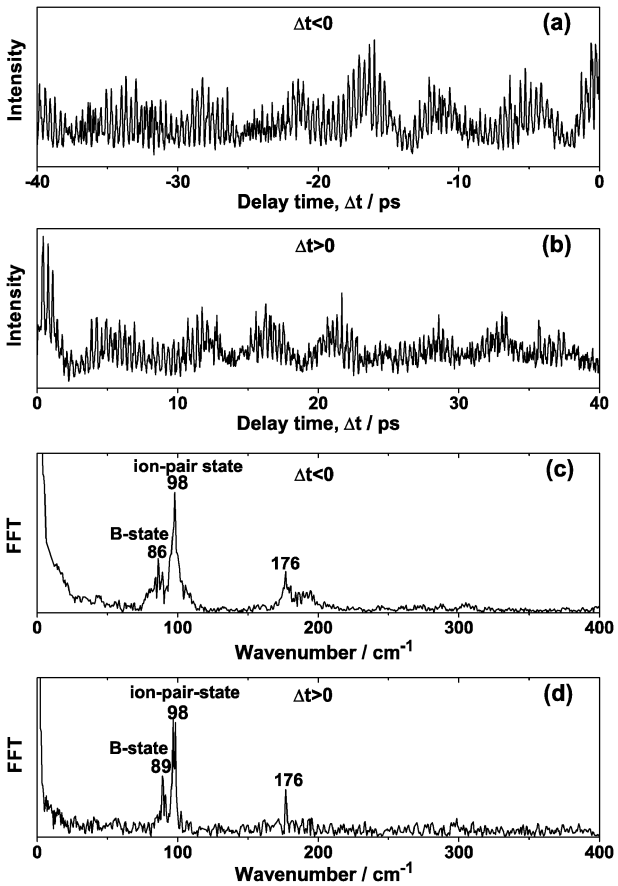

Fig. 3 DFWM transient obtained for an initial pump wavelength of 560 nm and a wavelength of 410 nm for the FWM laser pulses. Panels (a) and (b) show the DFWM signal recorded as function of the delay time Δt between the two time-coincident and fixed pump pulses and the probe pulse for negative and positive delay times, respectively. The initial pump pulse was made to arrive 42 ps earlier at the sample. Panels (c) and (d) show the FFT spectra of the transients for $\Delta t < 0$ and $\Delta t > 0$, respectively.

For $\Delta t > 0$ the two time-coincident DFWM pump pulses (pu_1 and pu_2) create a wave packet in the B state as well as in the ion pair state. These are then probed by the DFWM probe pulse (pr). The relevant energy level diagram for this is shown in panel (b) of Fig. 4. For positive time delays a superposition of B and ion-pair state signals can be observed in the resulting DFWM signal. The dynamics thus reveal the wave packet motion in the B state and in the ion pair state. In the FFT of the transients for $\Delta t > 0$ this is shown. Along with the B state contribution at 89 cm^{-1} there appears a sharp peak at 98 cm^{-1}, which belongs to the ion-pair state of the first tier. It is worth noting that for positive time delays, following the initial pump, the DFWM pump pulses are incident on the sample. Since the initial pump and DFWM pump pulses are fixed there is no change in timing between those. The DFWM probe pulse incident at successive time delays sees the wave

 This journal is © the Owner Societies 2008

View Article Online

Published on 10 December 2007. Downloaded by University of Pittsburgh on 27/10/2014 07:40:52.

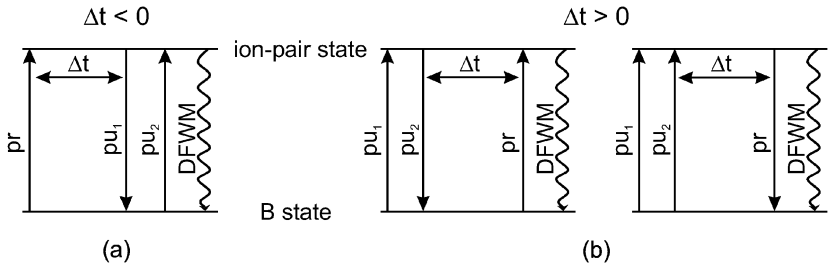

Fig. 4 Energy level diagrams corresponding to the DFWM processes taking place for $\Delta t < 0$ (a) and for $\Delta t > 0$ (b).

packet prepared by the DFWM pump pulses. Thus for $\Delta t > 0$ the wave packet prepared by the DFWM pump pulses solely contributes to the signal.

With the above experiments vibrational dynamics of the B state and ion pair states belonging to the first group were observed. However, it is of interest whether with the same technique ion pair states belonging to a different tier can also be accessed. For this, the wavelengths of the initial pump and FWM beams are changed to 540 and 343 nm, respectively. The total photon energy now corresponds to 47 673 cm^{-1}, which is above the potential energy minimum of the states $f(0_g^+)$ and $G(1_g)$ that can be accessed by a single photon transition from the excited B state. In the frequency domain these states are analyzed in detail.[25–28] However there are no studies carried out on these states in the time domain.

The experiments were performed as described before. Panel (a) of Fig. 5 shows the DFWM signal recorded as a function of time, ΔT between the initial pump and the time-coincident DFWM beams. The transient shows well-defined oscillations of the FWM signal for $\Delta T > 0$. For $\Delta T < 0$ a constant signal is observed which is the non resonant signal from the ground state. An FFT performed on the transient for $\Delta T > 0$ is shown in panel (b) of Fig. 5. Sharp peaks are observed in the region around 72 cm^{-1} in the FFT spectrum. This corresponds to the vibrational energy spacing in the excited B state accessed by the 540 nm laser. The second harmonic of this frequency is seen at around 144 cm^{-1}. With this experiment the dynamics of the excited B state are observed.

In order to reveal the dynamics of the ion pair states of the second tier, the experiments have to involve a time-resolved DFWM process as used before. The initial pump pulse is made to arrive 42 ps before the time coincident DFWM pump pulses are incident on the sample. The DFWM probe pulse is varied from negative to positive time delays while the two DFWM pump pulses were kept temporally overlapped and fixed at time zero. The transients recorded in this case are shown in panels (a) and (b) of Fig. 6 for negative and positive time delays of the probe pulse, respectively. Modulations of the DFWM signal are observed for negative and positive delay times. The data are analyzed by calculating the FFT. The result of this is shown in panel (c) of Fig. 6 for $\Delta t < 0$. The FFT spectrum shows peaks at 73, 101, and 144 cm^{-1}. The lines at 73 and 144 cm^{-1} are representatives of the excited B state. The line at 101 cm^{-1} is the vibrational energy spacing of the ion-pair state belonging to the second tier, which is accessed by the 540 and 343 nm lasers together. With the wavelengths used for the initial pump and DFWM beams potential energy surfaces in the higher energy region are accessed. In this region it should be noted that due to the anharmonicity of the well, the vibrational energy spacing is much smaller for states belonging to the first tier. Therefore, the intense line observed at 101 cm^{-1} cannot be attributed to states belonging to the first tier. However ion-pair states in the second group have comparable values in this energy range as is evident from Table 1. So clearly the 101 cm^{-1} line can be assigned to the ion pair state in the second group. As in the previous case, the B state signal observed for negative time delays is due to the varying time delay between the initial pump pulse and DFWM probe pulses. The FFT for positive time delay shows several lines. Again, the peak at 100 cm^{-1} clearly belongs to the ion-pair state. The second harmonic of this frequency is seen at

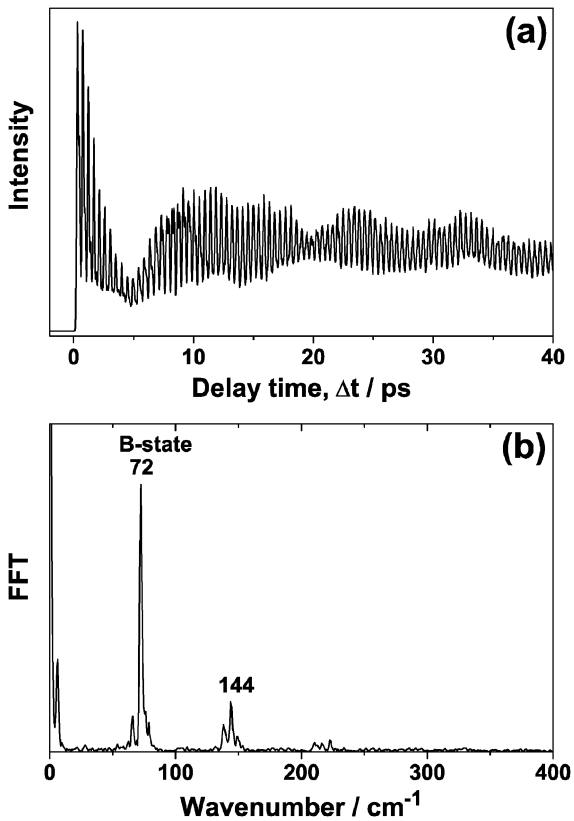

Fig. 5 Panel (a) shows the DFWM signal recorded as a function of the delay time ΔT between the initial pump (540 nm) and the three time-coincident FWM (343 nm) beams. Transients show oscillations with an approximate period of 463 fs. Panel (b) depicts the FFT spectrum of the transient in (a). It shows a peak at approximately 72 cm^{-1}, which corresponds to the vibrational energy spacing of the B state of molecular iodine accessed by the 540 nm laser.

View Article Online

Published on 10 December 2007. Downloaded by University of Pittsburgh on 27/10/2014 07:40:52.

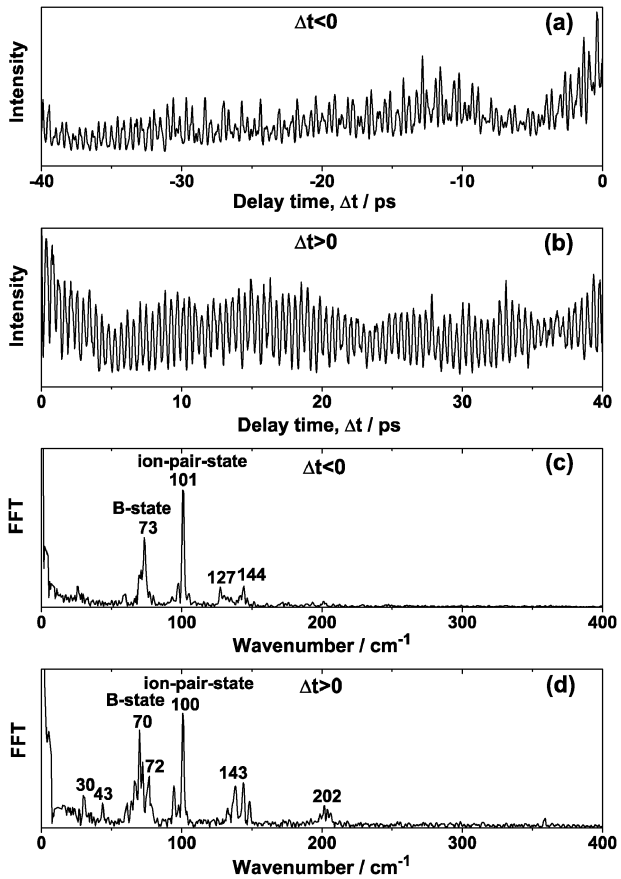

Fig. 6 DFWM transient obtained for an initial pump wavelength of 540 nm and a wavelength of 343 nm for the FWM laser pulses. Panels (a) and (b) show the DFWM signal recorded as function of the delay time Δt between the two time-coincident and fixed pump pulses and the probe pulse for negative and positive delay times, respectively. The initial pump pulse was made to arrive 42 ps earlier at the sample. Panels (c) and (d) show the FFT spectra of the transients for $\Delta t < 0$ and $\Delta t > 0$, respectively.

202 cm^{-1}. The peaks in the region of 70 and 143 cm^{-1} belong to the B state. Also the beatings between the different vibrational wavenumbers can be observed. The component at 30 cm^{-1} is the difference wavenumber between 70 and 100 cm^{-1} and the component at 43 cm^{-1} is the difference wavenumber between 100 and 143 cm^{-1}.

Experiments were also performed for different FWM wavelengths (325 and 335 nm) keeping the wavelength of the initial pump pulse fixed. In these experiments a decrease of the vibrational energy spacing of ion-pair state with higher photon energy was observed, which is consistent with expectations. Lower wavelengths access higher regions of the potential energy surface where the vibrational energy spacing is smaller. Since the spectroscopic constants of the ion pair state belonging to each tier are similar it is difficult to determine whether the contribution observed in the FFT spectrum is from the 0_g^+ or 1_g state. However, since the $\Delta\Omega = 0$ transition is more than an order of magnitude stronger than the $\Delta\Omega = 1$ transition, we assume that in our experiments only contributions from the 0_g^+ state are observed. So it is fair to conclude that in the experiments to explore the ion-pair states in the first and second tier the main contributions to the transients are from the $E(0_g^+)$ and $f(0_g^+)$ states, respectively.

4. Conclusions

Using a combination of an initial pump pulse and a time-resolved degenerate four-wave mixing (DFWM) process, we have shown that wave packet motion on different potential energy surfaces can be studied. This is demonstrated for iodine where, by having a proper choice of the wavelengths for the initial pump pulse and the DFWM pulses, wave packet motion in ion-pair states belonging to different tiers were observed. The dynamics corresponded well to the vibrational energy levels, which belong to the different electronic states. The technique presented offers access to the dynamics of high lying electronic states, which is of interest especially for more complicated molecular systems where processes like internal conversions play a role.

Acknowledgements

The authors thank Dr Torsten Balster for his help with the measuring software. This work has been supported by the German Research Foundation (Deutsche Forschungsgemeinschaft).

References

1 S. Mukamel, *Principles of Nonlinear Optical Spectroscopy*, Oxford University Press, Oxford, 1995.
2 R. Leonhardt, W. Holzapfel, W. Zinth and W. Kaiser, *Chem. Phys. Lett.*, 1987, **133**, 373.
3 M. Schmitt, G. Knopp, A. Materny and W. Kiefer, *Chem. Phys. Lett.*, 1997, **270**, 9.
4 M. Schmitt, G. Knopp, A. Materny and W. Kiefer, *Chem. Phys. Lett.*, 1997, **280**, 339.
5 M. Motzkus, S. Pedersen and A. H. Zewail, *J. Phys. Chem.*, 1996, **100**, 5620.
6 T. Siebert, M. Schmitt, A. Vierheilig, G. Flachenecker, V. Engel, A. Materny and W. Kiefer, *J. Raman Spectrosc.*, 2000, **31**, 25.
7 A. Materny, T. Chen, M. Schmitt, T. Siebert, A. Vierheilig, V. Engel and W. Kiefer, *Appl. Phys. B: Lasers Opt.*, 2000, **71**, 299.
8 E. J. Brown, Q. Zhang and M. Dantus, *J. Chem. Phys.*, 1999, **110**, 5772.
9 R. Leonhardt, W. Holzapfel, W. Zinth and W. Kaiser, *Rev. Phys. Appl.*, 1987, **22**, 1735.
10 C. C. Hayden and D. W. Chandler, *J. Chem. Phys.*, 1995, **103**, 10465.
11 M. Schmitt, G. Knopp, A. Materny and W. Kiefer, *J. Phys. Chem. A*, 1998, **102**, 4059.
12 R. S. Mulliken, *J. Chem. Phys.*, 1971, **55**, 288.
13 A. L. Guy, K. S. Viswanathan, A. Sur and J. Tellinghuisen, *Chem. Phys. Lett.*, 1980, **73**, 582.
14 K. P. Lawley and R. J. Donovan, *J. Chem. Soc., Faraday Trans.*, 1993, **89**, 1885.
15 J. P. Perrot, B. Femelat, J. L. Subtil, M. Broyer and J. Chevaleyre, *Mol. Phys.*, 1987, **61**, 85.
16 J. P. Perrot, B. Femelat, M. Broyer and J. Chevaleyre, *Mol. Phys.*, 1987, **61**, 97.
17 R. M. Bowman, M. Dantus and A. H. Zewail, *Chem. Phys. Lett.*, 1990, **174**, 546.
18 P. Farmanara, H. H. Ritze, V. Stert and W. Radloff, *Chem. Phys. Lett.*, 1999, **307**, 1.
19 P. P. Ho and R. R. Alfano, *Phys. Rev. A: At., Mol., Opt. Phys.*, 1979, **20**, 2170.
20 A. C. Eckbreth, *Appl. Phys. Lett.*, 1978, **32**, 421.

 This journal is © the Owner Societies 2008

View Article Online

21 T. Ishiwata and I. Tanaka, *Laser Chem.*, 1987, **7**, 79.
22 G. W. King, I. M. Littlewood and J. R. Robbins, *Chem. Phys.*, 1981, **56**, 145.
23 J. P. Perrot, M. Broyer, J. Chevaleyre and B. Femelat, *J. Mol. Spectrosc.*, 1983, **98**, 161.
24 R. F. Barrow and K. K. Yee, *J. Chem. Soc., Faraday Trans. 2*, 1973, **69**, 684.
25 K. S. Viswanathan, A. Sur and J. Tellinghuisen, *J. Mol. Spectrosc.*, 1981, **86**, 393.
26 U. Heemann, H. Knockel and E. Tiemann, *Chem. Phys. Lett.*, 1982, **90**, 17.
27 J. C. D. Brand and A. R. Hoy, *J. Mol. Spectrosc.*, 1983, **97**, 379.
28 E. Kagi, N. Yamamoto, H. Fujiwara, M. Fukushima and T. Ishiwata, *J. Mol. Spectrosc.*, 2002, **216**, 48.

Published on 10 December 2007. Downloaded by University of Pittsburgh on 27/10/2014 07:40:52.

Save valuable time searching for that elusive piece of vital chemical information.

Let us do it for you at the Library and Information Centre of the RSC.

We are your chemical information support, providing:

- Chemical enquiry helpdesk
- Remote access chemical information resources
- Speedy response
- Expert chemical information specialist staff

Tap into the foremost source of chemical knowledge in Europe and send your enquiries to

library@rsc.org

12120515

RSC Publishing

www.rsc.org/library